Published in final edited form as:
Biochim Biophys Acta. 2009 February ; 1793(2): 406–417. doi:10.1016/j.bbamcr.2008.09.011.

Agonist-dependent phosphorylation of the formyl peptide receptor is regulated by the membrane proximal region of the cytoplasmic tail

Elena S. Suvorova, **Jeannie M. Gripentrog**, **Algirdas J. Jesaitis**, and **Heini M. Miettinen***
Department of Microbiology, Montana State University, Bozeman, MT 59717, USA

Abstract

Formyl peptide receptor (FPR) is a chemoattractant G protein-coupled receptor (GPCR) involved in the innate immune response against bacteria. Receptor activation is terminated by receptor phosphorylation of two serine- and threonine-rich regions located in the distal half of the cytoplasmic tail. In this study we show that introduction of an amino acid with a bulky side chain (leucine or glutamine) adjacent to a single leucine, L320, in the membrane-proximal half of the cytoplasmic tail, significantly enhanced receptor phosphorylation, β-arrestin1/2 translocation, and receptor endocytosis, without affecting G_i-mediated ERK1/2 activation and release of intracellular calcium. In addition, the point mutations resulted in diminished susceptibility to trypsin, suggesting a conformation different from that of wild type FPR. Alignment of the FPR sequence with the rhodopsin sequence showed that L320 resides immediately C-terminal of an amphipathic region that in rhodopsin forms helix 8. Deletion of seven amino acids (Δ309–315) from the predicted helix 8 of FPR (G307–S319) caused reduced cell signaling as well as defects in receptor phosphorylation, β-arrestin1/2 translocation and endocytosis. Thus, the amino acid content in the N-terminal half of the cytoplasmic tail influences the structure and desensitization of FPR.

Keywords

Chemoattractant receptor; cell signaling; desensitization; protein folding; cytoplasmic helix 8

INTRODUCTION

Chemoattractant receptors N-formyl peptide receptor (FPR) and the anaphylatoxin C5a receptor (C5aR), belong to a family of rhodopsin-like G protein-coupled receptors (GPCR) [1]. Binding of exogenous or endogenous N-formylated peptides to FPR, and complement C5a fragment to C5aR, results in neutrophil migration from the bloodstream to sites of infection or tissue injury. Upon exposure to agonist, both receptors undergo a conformational change that enables binding and activation of G protein. Inactivation of GPCRs is a multistep process involving phosphorylation of the cytoplasmic tail, binding of β-arrestin1/2, and receptor endocytosis. The phosphorylation takes place on serine and threonine residues in a ligand concentration-dependent and time-dependent manner. The phosphorylated residues produce a localized concentration of negative charges that provide one of the binding sites for ß-arrestin; the other binding site is provided through the ligand-binding-induced conformational change in the receptor [2].

*Corresponding author: Department of Microbiology, Montana State University, 109 Lewis Hall, Bozeman, MT 59717, USA., Tel.: +1-406-994-4014; Fax: +1-406-994-4926. E-mail address: E-mail: heini@montana.edu.

We have previously shown that a dileucine, L318/L319, in the membrane proximal region of the cytoplasmic tail of C5aR is important for receptor conformation, phosphorylation and endocytosis [3]: Mutagenesis of leucine 319 into alanine caused protein retention in the endoplasmic reticulum (ER) of transfected Chinese hamster ovary (CHO) cells, possibly due to improper protein folding recognized by the quality control system of the ER [4]. The exchange of leucine 318 to alanine did not affect protein transport to the plasma membrane, but caused a defect in receptor phosphorylation, which in turn reduced receptor internalization [3]. Furthermore, a comparison of limited proteolysis of wild type C5aR and the C5aR L318A mutant expressed in CHO cells showed different sensitivity to digestion with trypsin, suggesting a structural difference between the wild type and mutant receptor. Thus, the intact dileucine was essential for a protein structure that supports normal receptor function. (Although dileucines are fairly commonly described as part of an export and/or internalization signal in GPCRs, the C5aR sequence does not conform to the classical dileucine-based motifs [5]).

Based on the importance of the dileucine in the function of C5aR, one might expect that FPR also contains a dileucine in the corresponding location of the cytoplasmic tail. However, despite 38% identity and 52% similarity between the cytoplasmic tails of FPR and C5aR, FPR contains only one leucine (L320) corresponding to L319 in C5aR [6,7]. Since we have previously observed that the rate of ligand-induced phosphorylation and endocytosis of FPR is slower than that of C5aR, we examined whether the introduction of a dileucine in the corresponding site in FPR (L319/L320, L320/L321) would increase the rate of phosphorylation. The results from our previous study with C5aR also supported a model in which the L318/L319 dileucine in C5aR stabilized a putative amphipathic helix 8 in the membrane-proximal region of the cytoplasmic tail. Therefore, we examined the effect of a seven amino acid deletion (Δ309–315) in the putative helix 8 of FPR on receptor phosphorylation, ß-arrestin1/2 recruitment and receptor endocytosis. The results from these studies suggested that helix 8 is required for normal receptor function supported by a dileucine that promotes rapid receptor phosphorylation, ß-arrestin1/ 2 binding and receptor endocytosis. Finally, limited proteolysis with trypsin further corroborated a conformational difference between wild type FPR and the FPR dileucine mutants. Together, the results from this study lend further support to our hypothesis that phosphorylation of GPCRs is in part regulated by receptor conformation involving helix 8 and surrounding residues.

MATERIALS AND METHODS

Reagents and antibodies

f-Methionine-leucine-phenylalanine (fMLF)was purchased from Sigma-Aldrich (St Louis, MO). Trypsin Gold, Mass spectrometry grade was obtained from Promega Corporation (Madison, WI). Endoglycosidase H (Endo H) and N-glycosidase F (PNGase F) were obtained from New England Biolabs Inc. (Ipswich, MA). Enhanced chemiluminescence (ECL) reagents were from Perkin-Elmer Life Sciences (Boston, MA). Rabbit monoclonal anti-phospho-p44/42 MAPK (Thr202/Tyr204) (197G2) antibody was obtained from Cell Signaling Technology Inc. (Danvers, MA), and rabbit polyclonal anti-p44/42 MAPK antibody was from Upstate Cell Signaling Solutions (Lake Placid, NY). Monoclonal antibody (mAb) NFPR1 and NFPR2 against FPR were described previously [8]. Rabbit polyclonal antibody against β-arrestin1/2 was a gift from Robert Lefkowitz (Howard Hughes Medical Institute and Duke University Medical Center, Durham, NC). Horseradish peroxidase (HRP) conjugated goat anti-mouse and anti-rabbit antibodies were purchased from Jackson ImmunoResearch Laboratories Inc. (West Grove, PA). Alexa™488-conjugated goat anti-mouse was obtained from Molecular Probes Inc. (Eugene, OR).

Oligonucleotide-directed mutagenesis of FPR and CHO cell transfection

Point mutations of human FPR ([9]; cDNA clone R-26; GenBank accession no M60627) were generated by oligonucleotide-directed mutagenesis using single-stranded DNA template and confirmed by DNA sequencing (Nevada Genomics Center, University of Nevada–Reno). cDNAs with a mutation were inserted into pBGSA expression vector (GenBank accession number AY6607190), which confers G418 resistance [10]. Constructs were transfected into Chinese hamster ovary (CHO) cells using Lipofectamine™2000 transfection reagent (Invitrogen Life Technologies) according to the manufacturer's recommendations. CHO cells were cultured in α-modified Eagle's medium (α-MEM; Sigma) supplemented with 5% fetal bovine serum (FBS), 50 units/ml penicillin and 50 μg/ml streptomycin. Stable transfectants were selected with 0.5 mg/ml G418. Twelve to sixteen single colonies were tested for receptor expression and cellular localization by immunofluorescence microscopy. Clones of each mutant with expression levels similar to the wild type receptor were chosen for further study.

Indirect immunofluorescence microscopy

CHO transfectants were grown on glass coverslips. In endocytosis experiments, cells were incubated for 0, 10 or 60 min at 37°C with 100 nM fMLF before fixation with methanol (mAb NFPR1 does not bind FPR fixed with paraformaldehyde). Incubations with primary mAbs NFPR1 and NFPR2 (10 μg/ml) and secondary antibody Alexa™488-conjugated goat anti-mouse IgG (1:600) were carried out for 1 h at room temperature. The coverslips were mounted in 2.5 mg/ml DABCO/Glycergel (Sigma) and viewed using a 63× objective on an Axioskop microscope (Carl Zeiss Inc., Thornwood, NY). The digital images were adjusted and cropped in Adobe Photoshop.

Endoglycosidase H and PNGase F digestion

CHO transfectants were scraped from tissue culture plates in PBS containing a protease inhibitor cocktail (1:1000; P8340, Sigma-Aldrich) and 1 mM phenyl methyl sulfonyl fluoride (PMSF). Cells were sedimented by centrifugation, suspended in glycoprotein denaturation buffer, and denatured for 10 min at 80°C (higher temperatures cause aggregation of FPR). Samples were divided into three tubes and incubated without enzyme or with Endo H or PNGaseF, according to the manufacturer's instructions. Undigested and digested FPR were detected by western blot analysis and ECL using mAb NFPR2 and HRP-conjugated secondary antibody.

Western blot analysis of FPR phosphorylation

Cells were grown on 35 mm dishes and induced overnight with 6 mM Na butyrate. Cells were stimulated with 100 nM fMLF for 0, 1, 3, 10 or 30 min, or for 5 min with 0, 1, 3, 10, 30, 100, 300, 1000 or 3000 nM fMLF, rinsed with cold PBS and collected in PBS with 1 mM PMSF and a phosphatase inhibitor cocktail (1:100, P2850, Sigma-Aldrich). After sonication, membranes were sedimented by centrifugation at 21,000 × g, 20 min, 4°C. Membranes were solubilized in Laemmli sample buffer [11] for 20 min at 60°C, and FPR was detected and quantified by conventional western blot analysis or by blot dot analysis. In conventional western blot analysis, proteins were separated on a SDS-10% polyacrylamide gel and transferred to a 0.45 μm nitrocellulose membrane using a semi-wet unit (Bio-Rad). In dot blot analysis, samples were pipetted onto nitrocellulose membranes, dried, and incubated in transfer buffer for 5 min. Western blot and dot blot membranes were briefly stained in 0.1% Ponceau S in 3% glacial acetic acid to confirm equal protein loading. The membranes were blocked in 10% non-fat dry milk in Tris-buffered saline with 0.5% Tween-20 (TBST) for at least 1 h. After washes with PBS, the membranes were incubated with primary antibody in TBST containing 5% BSA for 1 h at room temperature or overnight at 4°C. Total FPR was detected with mAb NFPR1 and non-phosphorylated FPR was detected with mAb NFPR2. ECL was

carried out as above. The relative quantity of the proteins was calculated after scanning using Scion image software (Scion Corporation, Frederick, MA).

β-Arrestin1/2 assay

Cells grown on 60 mm dishes were stimulated for 5 min with various concentrations of fMLF (0, 1, 3, 10, 30, 100, 300, 1000 and 3000 nM). After washing with cold PBS, cells were removed by scraping in 1 ml PBS containing protease inhibitor cocktail (1:1000) and 1 mM PMSF. Cell suspension was sonicated and the membranes were sedimented by centrifugation for 15 min 21,000 × g, 4°C. The proteins from the cytosol-containing supernatant were precipitated by centrifugation in 70% ethanol and both membrane and cytosol pellets were solubilized for 20 min at 60°C in Laemmli sample buffer followed by sonication. β-Arrestin1/2 was detected by western blot analysis and quantified as above. Data were analyzed by non-linear regression analysis using Prism 3.0 software (GraphPad Software, San Diego, CA).

Flow cytometry

To measure the relative amount of wild type and mutant FPRs expressed in the CHO transfectants, cells were incubated for 1 h on ice in the presence of 40 nM formyl-Norleucine-Leucine-Phenylalanine-Norleucine-Tyrosine-Lysine-fluorescein (f-NleLFNleYK-fluorescein; Molecular Probes Inc.). Nonspecific binding was determined in the presence of 40 μM fMLF. Ten thousand cells were analyzed using FACScan flowcytometer and nonspecific binding was subtracted from total binding. The relative surface expression levels of the mutant receptors were calculated as percentage of wild type receptor.

The ligand binding K_d values were calculated as previously described [12]. Briefly, cells were incubated on ice with 50 pM to 40 nM f-NleLFNleYK-fluorescein in the absence or presence of 1000-fold excess fMLF (background). Cells were analyzed in a FACScan flow cytometer and the K_d values were determined by least squares analysis of the mean fluorescence intensity using the Prism software.

To measure receptor internalization, CHO transfectants were incubated for 15 min with or without 100 nM fMLF and washed with cold PBS pH 3.0 to remove cell surface ligand. FPR on the cell surface was detected by FACScan analysis after 45 min incubation on ice with 20 nM f-NleLFNleYK-fluorescein ± 20 μM fMLF.

ERK1/2 activation assay

CHO transfectants were induced overnight with 6 mM Na butyrate and pre-incubated in serum-free medium for 2 h to reduce ERK1/2 activation by growth factors in the serum. Cells were stimulated with 100 nM fMLF for 0, 2, 5, 10 or 30 min, or for 5 min with 0, 0.1, 0.5, 1.0, 5.0 or 10.0 nM fMLF, rinsed with cold PBS and collected in Laemmli sample buffer. Cell lysates were analyzed in western blots using rabbit anti-total ERK1/2 and anti-phospho-ERK1/2 antibodies.

Ca^{2+} mobilization assay

CHO transfectants were induced overnight with 6 mM Na butyrate, and removed by scraping from tissue culture dishes incubated in Ca^{2+}/Mg^{2+} - free PBS containing 1 mM EDTA, pH 8.0. Cells were loaded with 2.5 nM Fura 2-AM (Molecular Probes Inc.) in PBS with 5% FBS. Release of intracellular Ca^{2+} in response to 0.05, 0.1, 0.25, 0.5, 1 and 5.0 nM fMLF or 1, 5, 10, 25, 50 and 100 nM fMLF (FPR Δ309–315) was detected using a double-excitation monochromator fluorescence spectrofluorometer, as previously described [13]. The chosen fMLF concentrations resulted in a range of Ca^{2+} release from barely detectable to maximal or near maximal. To determine EC_{50} values, the relative amount of fMLF-induced calcium release

was calculated by subtracting the baseline from the fMLF peak value. 10 μM ATP was added as a heterologous ligand to provide a standard stimulus for calcium mobilization. Data were analyzed by non-linear regression analysis using Prism 3.0 software, as previously described [13].

Limited proteolysis with trypsin

CHO cells expressing wild type and mutant FPR were collected in PBS containing 1 mM PMSF. After sonication, membranes were sedimented at 21,000 × g for 20 min at 4°C and solubilized in 1% Triton X-100 in sterile PBS on ice for 1 h. Trypsin stock solution and dilutions were made according to the manufacturer's recommendation (Promega Inc., Madison, WI). CHO membranes in duplicates were treated with increasing concentrations (0–10 ng/μl) of trypsin for 1 h at room temperature. Proteolysis was stopped by placing samples on ice for 10 min, adding Laemmli sample buffer and heating at 60°C for 5 min. Receptor proteolysis was detected by western blotting using mAb NFPR2. Data were analyzed by non-linear regression analysis using Prism 3.0 software.

RESULTS

The central part of the cytoplasmic tail of FPR is critical for transport to the cell surface

To examine the role of the FPR cytosolic tail in receptor function, we generated a number of deletion and point mutations and expressed the receptors in Chinese hamster ovary (CHO) cells (Figure 1 and Table 1). First we analyzed the cellular localization of the deletion mutants by immunostaining of the cells with anti-FPR antibodies. Seven residue deletions in the middle of the cytoplasmic tail (FPR Δ316–322 and FPR Δ323–329) resulted in intracellular retention of the receptor (Figure 2A). Another deletion mutation (FPR Δ309–315) was transported to the cell surface, although immunofluorescence staining also suggested minor intracellular localization. FPR Δ309–315 was not recognized by mAb NFPR1, corroborating phage display peptide analysis results that mapped the antibody binding sites to residues 306–313 [8]. The intracellular retention of FPR Δ316–322 and FPR Δ323–329 was further confirmed by digestion of their N-linked glycans. N-glycosylated proteins that are retained in the endoplasmic reticulum (ER) can be identified by their sensitivity to endoglycosidase H (Endo H), an enzyme that cleaves only unprocessed N-linked glycans characteristic of the ER. After modifications in the Golgi complex, the N-glycans become resistant to cleavage with Endo H, but can be digested by endoglycosidase F (PNGase F). As shown in Figure 2B, the N-linked glycans on FPR Δ316–322 and FPR Δ323–329 were Endo H sensitive and the undigested receptors migrated significantly faster through the SDS-polyacrylamide gel than wild type receptor, suggesting that the N-glycans were not fully processed and therefore had not passed through the Golgi complex. Deletion of the membrane proximal seven amino acids (309–315) and mutagenesis at positions 318, 319 and 321 (discussed in more detail below) did not prevent transport of the mutant receptors to the cell surface (Figure 2B). Therefore, we conclude that the middle portion of the FPR carboxyl tail is likely to play a critical role in maintaining a functional receptor conformation.

Accelerated phosphorylation of FPR mutants bearing a bulky residue next to L320

We recently demonstrated that a dileucine (L318/L319) in the membrane proximal region of the carboxyl tail of the C5a receptor (C5aR) is important for receptor phosphorylation and folding [3]. Examination of the amino acid sequence of the FPR tail showed a high similarity with the tail of C5aR, particularly in the membrane proximal area (Figure 8). However, a notable difference between the two receptors is the dileucine found in C5aR (L318/L319), but lacking from FPR (L320). We therefore generated FPR dileucine mutants with the second leucine introduced to the site analogous to C5aR L318 (FPR S319L) or immediately after the single leucine (FPR E321L) (Figure 1). We also generated a double FPR mutant A318S/S319L

(Figure 1) that contained a continuous stretch of five amino acids in common with C5aR (315-LPSLL-319). Since the membrane proximal region of the C5aR is positively charged, we also generated a FPR E321Q mutant to investigate the effect of removing a negative charge (E) from the area.

To analyze FPR phosphorylation, we took advantage of monoclonal anti-FPR antibodies, NFPR1 and NFPR2 [8]. The binding site for mAb NFPR2 was mapped to the distal part of the carboxyl tail, S338–V345, which includes two major phosphorylation sites, S338 and T339. We have previously shown that ligand-induced phosphorylation of FPR resulted in reduced mAb NFPR2 binding to the receptor [8]. The reduction of mAb binding was time- and fMLF concentration-dependent and could be reversed by exposing CHO FPR membranes to shrimp alkaline phosphatase, indicating that the loss of antibody binding was indeed due to receptor phosphorylation, rather than some other physiological change [8]. Thus, we used mAb NFPR2 as a tool to follow phosphorylation of wild type and mutant FPRs. As mentioned above, mAb NFPR1 has a major binding site in the membrane proximal region of the cytoplasmic tail (Q306–I313) and recognizes phosphorylated and non-phosphorylated receptor equally well. To quantitatively compare phosphorylation of the mutants with the wild type receptor, we used a dot blot technique that allows simultaneous analysis of a large number of samples. The western blots and the dot blots in Figure 3A and B show the time course of phosphorylation in CHO transfectants expressing wild type FPR and the FPR E321L mutant in the presence of 100 nM fMLF. Wild type FPR shows minor phosphorylation (decrease in mAb NFPR2 binding) at 1 and 3 min, whereas phosphorylation of FPR E321L is more pronounced; the difference is clearly visible after 10 and 30 min incubation. Quantification of the receptors with the NFPR2 antibody showed that all mutants with a leucine on either side of L320 were more efficiently phosphorylated than the wild type receptor (Figure 3C). On the other hand, deletion of amino acids 309–315 completely blocked receptor phosphorylation, suggesting that this region of the receptor is required for normal receptor function (Figure 3C).

To further investigate the phosphorylation, the CHO transfectants were stimulated for 5 min with increasing concentrations of fMLF. Consistent with the time course data, all receptors containing a bulky residue around L320 showed a similar dose-dependence of phosphorylation with EC_{50}s ranging from 7.0 nM (FPR E321Q) to 21.1 nM (FPR S319L), whereas wild type FPR required a significantly higher concentration for maximal phosphorylation, with in an EC_{50} of 297 nM fMLF (Figure 4). Thus, an increase in hydrophobicity in close proximity to L320 (S321L, A318S/S319L, E321L) appeared to enhance receptor phosphorylation. The 1.5–3 fold lower EC_{50} for the FPR E321Q and FPR E321L mutants, compared to the other dileucine mutants, suggests that phosphorylation of FPR may be inhibited by the negative charge at position 321. Removal of the negative charge in combination with the retention of a bulky side chain (FPR E321Q) appeared to be most favorable for FPR phosphorylation.

To rule out the possibility that the introduced mutations increased ligand binding, thereby accelerating receptor phosphorylation, we determined the receptor K_ds (Table 1). The mutants showed similar binding affinities as wild type FPR. Thus, we conclude that, similar to C5aR, the membrane proximal region of the FPR tail is involved in regulation of receptor phosphorylation in the distal portion of the carboxyl tail.

Ligand-dependent interaction of the FPR mutants with β-arrestin1/2

Agonist-dependent phosphorylation of many GPCRs is considered the main regulator of receptor interaction with cytoplasmic scaffolding proteins, β-arrestin1 and 2. Studies of serine and/or threonine mutants of FPR have demonstrated a complex regulation of FPR phosphorylation and its effect on ß-arrestin1/2 binding [15,16]. We decided to examine how the FPR mutations that enhanced receptor phosphorylation would affect the interaction of FPR with ß-arrestin1/2. CHO transfectants were activated for 5 min with different concentrations

of fMLF. ß-Arrestin1/2 translocation to the cell membrane was monitored by western blot analysis and the quantitative results are summarized in Figure 5. All point mutants showed EC_{50} values lower than the wild type receptor, corresponding to the results obtained in the phosphorylation experiments. The difference between the wild type receptor and the A318S/S319L, E321L and E321Q mutants was statistically significant ($P < 0.05$), but less dramatic than the difference detected in phosphorylation. Thus, the mutations in the membrane proximal region of the cytosolic tail that resulted in enhanced phosphorylation also led to enhanced binding of ß-arrestin1/2. In the case of the phosphorylation deficient FPR Δ309–315 mutant, we expected to see no ligand-induced binding of ß-arrestin1/2 to the membrane fractions. This was indeed the case, as shown in Figure 5C, but the amount of ß-arrestin1/2 in the membrane fraction compared to the cytosol fraction was about the same in the absence of ligand (0 nM fMLF; 40 ± 7%) as in the presence of ligand (10 μM fMLF; 43.7 ± 6.2%). The equivalent numbers for wild type FPR were 18 ± 5 (0 nM) and 57 ± 9 (10 μM) [13]. Since FPR Δ309–315 does not become phosphorylated, we hypothesize that the deletion of these seven amino acids, none of which is a phosphoacceptor serine or threonine, results in a receptor conformation that is favorable for ß-arrestin1/2 interaction in the absence of phosphorylated amino acids. This finding also suggests that the lack of receptor phosphorylation may be at least in part due to the constitutively bound ß-arrestin1/2, which may sterically inhibit the interaction of other proteins such as G protein and G protein-coupled receptor kinase (GRK).

Mutation of the membrane-proximal region of FPR leads to enhanced agonist-dependent internalization

Internalization of a vast majority of GPCRs requires receptor phosphorylation, which induces conformational changes necessary for specific interactions of the GPCR with the endocytic machinery. We previously showed that a L318A mutation in the carboxyl end of the putative helix 8 of C5aR resulted in reduced phosphorylation and internalization [3]. Since reciprocal mutations in the FPR C-tail caused accelerated phosphorylation of the receptor, we examined the possibility that this would also enhance receptor endocytosis. First we measured the endocytosis by FACScan analysis: Cells were exposed to 100 nM fMLF for 15 min, washed, and the receptors remaining on the cell surface were measured using a fluorescein-conjugated formylated peptide (f-NleLFNleYK-fluorescein). As shown in Figure 6A, all point mutants had less FPR on the cell surface than the wild type receptor, suggesting more efficient endocytosis ($P < 0.01$, one-way ANOVA). In contrast, the FPR Δ309–315 mutant showed no evidence of endocytosis, corresponding to lack of ligand-induced phosphorylation and β-arrestin translocation.

Next we examined endocytosis by immunofluorescence microscopy. Immunofluorescence with mAb NFPR1 detected only minor differences between wild type FPR and the mutants, partly because the antibody binds both cell surface receptors and internalized receptors, and the former outshines the latter (Figure 6B). On the other hand, mAb NFPR2, which does not bind phosphorylated receptor, showed a large difference in staining pattern between wild type FPR and the mutants after 10 min exposure to ligand (Figure 6C). Whereas wild type FPR appeared to localize at least partly on the cell surface, the mutants demonstrated very little staining on the plasma membrane and showed predominantly perinuclear staining (Figure 6C). This suggests that most of the mutant receptors on the cell surface after 10 min stimulation were phosphorylated and did not bind the antibody. The receptors that had been endocytosed and dephosphorylated represented the majority of the non-phosphorylated receptor. Prolonged continuous exposure (60 min) to the ligand eliminated the difference, suggesting that a large proportion of wild type FPR had been phosphorylated on the cell surface and/or endocytosed and dephosphorylated during the 60 min incubation. In contrast, FPR Δ309–315 mutant maintained non-phosphorylated FPR on the cell surface even after 60 min exposure to ligand (Figure 6C). Therefore, the point mutations in the membrane proximal region of FPR

cytoplasmic tail that resulted in increased phosphorylation and β-arrestin1/2 binding, also led to enhanced receptor internalization.

FPR point mutations do not affect G protein-mediated cell signaling

To examine whether the enhanced receptor phosphorylation is due to changes in intracellular signaling pathways downstream of G_i, we examined two major signaling pathways; activation of the downstream kinases ERK1/2, and release of intracellular Ca^{2+}. Activated (phosphorylated) ERK1/2 was detected in western blots of whole cell extract after cells were stimulated with 100 nM fMLF for 0, 2, 5, 10 or 30 min. Both wild type and mutant receptors showed similar time-dependent activation of ERK1/2, reaching maximal activation at ~5 min (Figure 7A). Upon cell exposure to 0.1, 0.5, 1.0, 5.0 and 10 nM fMLF for 5 min, a similar concentration-dependence of ERK1/2 activation was observed between the different CHO transfectants (Figure 7B). Only FPR Δ309–315 showed a small delay in phosphorylation of ERK, possibly due to increased constitutive β-arrestin1/2 binding (Figure 5C), which may result in reduced binding of G_i [12].

We also examined signaling of wild type and mutant FPR by measuring the EC_{50} for ligand-binding-induced intracellular calcium release. Cells were loaded with Fura 2-AM and intracellular calcium release in response to various concentrations of fMLF was examined. Representative calcium curves for CHO FPR wild type and CHO FPR E321L are shown in Figure 8, and the combined results for all receptors are presented in Table 2. All CHO FPR mutants with enhanced phosphorylation showed a similar EC_{50} for calcium release compared to wild type FPR (mean values 0.11–0.22 nM), suggesting that the point mutations did not alter the G protein signaling capacity of the receptor, an event that takes place prior to receptor phosphorylation and β-arrestin1/2 binding. The FPR Δ309–315 mutant required significantly higher concentrations of fMLF to induce calcium release (EC_{50} = 1.7 ± 1.0 nM), again corroborating our previous results of reduced G protein coupling [12].

Tryptic cleavage data suggest that the FPR mutants are structurally different from the wild type receptor

The crystal structures of rhodopsin and β2-adrenergic receptor revealed the presence of a short amphipathic helix in the membrane-proximal part of the carboxyl tail of these GPCRs [17, 18]. Alignment of this region of rhodopsin with FPR (and C5aR) showed significant similarity in amino acid sequence, suggesting the presence of a similar structure in FPR (Figure 9A). Computational prediction analysis of the amino acid sequence using PSIpred (http://bioinf.cs.ucl.ac.uk/psipred/psiform.html) [19] and APSS2 (http://imtech.res.in/raghava/apssp/) servers predicted an α-helix from Q306 to S319 (Figure 9).

The structure of the carboxyl tail of most other GPCRs is mostly unknown due to high domain flexibility. Limited digestion of extracted membrane proteins with trypsin has been used successfully to study folding of membrane proteins [20]. We therefore decided to compare wild type FPR and the FPR point mutants by analyzing their sensitivity to trypsin. Receptors were extracted from membranes with Triton X-100 and subjected to digestion with increasing concentrations of trypsin. FPR degradation was detected by western blot analysis. Wild type FPR was more susceptible to trypsin than the analyzed mutants (Figure 10A and B). Degradation of the full-length wild type FPR led to accumulation of lower molecular weight bands of the receptor (Figure 10A and B). All mutants required two- to four-fold higher concentrations of trypsin to obtain degradation comparable to wild type FPR. This observation suggests that the tryptic cleavage sites are less accessible in the mutants, implicating a difference in receptor folding.

DISCUSSION

Structural studies of different members of the GPCR family have demonstrated that conformational changes play an important role in the functional regulation of the receptor. Agonist binding to extracellular loops and transmembrane domains results in an active receptor conformation which allows further interaction with intracellular partners. Despite many years of intensive study, the secondary structure of the cytosolic regions of GPCRs is still largely unknown due to their high flexibility. The carboxyl tails of the rhodopsin-like GPCRs represent the longest intracellular domains and bear functionally important phospho-acceptor amino acid residues, serines and threonines. In this study we demonstrated that agonist-induced phosphorylation of distal sites on FPR is regulated by structural determinants located in the membrane-proximal region of the tail. Targeted mutagenesis within this region just C-terminal of the predicted helix 8 revealed the critical importance of the amino acid content for the structural and functional regulation of the receptor.

Despite high similarity between C5aR and FPR, these two rhodopsin-like receptors display significant differences in their function [21]. Most relevant to the current study is our observation that in transfected CHO cells, C5aR becomes maximally phosphorylated more rapidly (~5 min) than FPR (~30 min) despite similar K_ds (10 nM C5a and 6 nM fMLF, respectively) [12,21] and this study). We also showed that disruption of the membrane-proximal dileucine of C5aR resulted in a decrease in receptor phosphorylation and endocytosis. The carboxyl tail of FPR shows 38% amino acid identity with C5aR, but does not contain the analogous dileucine. Introduction of the reciprocal mutations into FPR resulted in enhanced phosphorylation and endocytosis. Although K_d values for ligand binding to the dileucine mutants were similar to wild type FPR, the mutant receptors became more rapidly phosphorylated and required a lower ligand concentration for maximal phosphorylation (Figure 3). The increase in phosphorylation correlated with increased ß-arrestin1/2 binding and receptor endocytosis (Figure 4–Figure 6). The increased rate of phosphorylation did not appear to be due to differences in common signaling pathways, since early (2–5 min) activation of ERK1/2 and release of intracellular calcium in response to ligand gave similar results in CHO cells expressing wild type and dileucine mutant receptors (Figure 7 and Figure 8, Table 2). Thus, these findings led us to conclude that introduction of a dileucine (S319L/320L; 320L/E321L) or an additional bulky side chain (320L/E321Q) into FPR on a site analogous to the C5aR dileucine may play a significant role in promoting a receptor structure favorable for ligand-induced phosphorylation and endocytosis.

Analysis of the sequence in the proximal part of FPR and C5aR tails suggested the presence of an amphipathic helix similar to helix 8 of rhodopsin (Figure 9). Structural stability of the rhodopsin helix 8 is partly maintained by the presence of one or several cysteines at the COOH-terminus of the helix [17,22,23]. Lipid modification of these cysteines provides a membrane anchor that helps orient the short amphipathic helix toward the membrane. However, GPCRs from several sub-families, including FPR and C5aR do not have cysteines in the corresponding region, suggesting some other mechanism of membrane interaction. For example, the presence of positively charged and/or hydrophobic residues at the carboxyl end of helix 8 would draw the helix to the negatively charged lipid heads in the membrane. Thus, proteins containing an amphipathic helical binding motif do not show strict specificity for one lipid, but respond more generally to a negative charge. Membrane attachment via lipid anchor may provide a means of partitioning the protein into a certain microdomain such as lipid rafts [24,25]. The amphipathic helix of FPR is neutral overall and thus does not provide a strong interaction with the membrane. The presence of readily phosphorylated serines on the basic patch raises the possibility of easy helix detachment from the membrane. Phosphorylation of these serines will increase the concentration of negatively charged residues on the cytosolic face and may lead to repulsion of the helix from the membrane upon receptor phosphorylation. Introduction of

the second bulky hydrophobic residue, leucine, at the COOH-terminus of helix 8 could result in a stronger interaction of the helix with the membrane. In addition, elimination of the serine in FPR S319L, and glutamic acid in FPR E321L and FPR E321Q would reduce the negative charge in the area, further promoting the interaction with the membrane. Thus, all the point mutations that were introduced to the cytoplasmic tail of FPR have the potential to increase the proximity of the N-terminal part of the cytoplasmic tail to the plasma membrane. This receptor conformation may favor interaction with intracellular binding partners, such as GRK2, which interacts with the membrane through a lipid modification and has been shown to phosphorylate FPR [26].

The requirement of receptor phosphorylation in ß-arrestin1/2 binding may be variable among different GPCRs. Phosphorylation of non-visual GPCRs generally results in 2- to 3-fold increase in ß-arrestin, but a bulk negative charge acting as a phosphomimetic may be as important as the phosphorylated serine or threonine residue in binding of the positively charged recognition domain on ß-arrestin [2]. FPR Δ309–315 has a slight increase in the net negative charge due to loss of two positive charges (R309 and R311) (and one negative charge [E310]). This increase in negative charge could possibly affect the affinity of s-arrestin and explain the increased amount of ß-arrestin in the membrane fraction of cells expressing this non-phosphorylated mutant. The identity and relative position of the phospho-acceptor amino acids are also important factors in ß-arrestin binding, as would be expected: Mutagenesis studies of FPR showed that two domains containing serine and threonine residues (S328–S332 and T334–T339) are required for FPR internalization and desensitization [27], and further analysis pinpointed phospho-S328, -S332, and -S338 as critical for ß-arrestin binding, internalization, and desensitization [16]. The high affinity binding of ß-arrestin to FPR was shown to be highly regulated by the phosphorylation status of S328–S332, while phospho-T334-T339 were more important for endocytosis [14,16]. Our results show that FPR mutants S319L, E321L, E321Q and A318S/S319L all enhanced receptor phosphorylation, ß-arrestin binding, and endocytosis. Thus, the combination of two hydrophobic bulky side chains (LL) or one hydrophobic and one neutrally charged side chain (LQ) immediately C-terminal of putative helix 8, and 7–8 residues N-terminal of S328 appear to increase the rate of interaction with GRK, suggesting a conformational difference. This hypothesis was further supported by the finding that wild type FPR was more susceptible to proteolytic digestion with trypsin than the mutant receptors (Figure 10).

Mutagenesis studies of several GPCRs, including rhodopsin, protease-activated receptors, and β1-adrenergic receptor, have shown that helix 8 is directly involved in G protein coupling [28–31]. We have previously shown that ligand binding to FPR Δ309–315 resulted in 50% reduction in G protein coupling [12]. In this study, we show that the mutant receptor is also impaired in receptor phosphorylation, β-arrestin1/2 binding, receptor endocytosis, and signaling. Thus, our data are consistent with previous results suggesting a direct contact of helix 8 with the membrane-associated region of G protein α and γ subunits [28–31]. In addition, this study and our previous study using C5aR mutants, suggest that helix 8 and adjacent amino acids coordinate receptor phosphorylation independently of receptor signaling.

As the number of studies on GPCR activation, signaling and desensitization steadily increases, so does our understanding of the common and receptor-specific structural elements that are involved in the regulation. With the known detrimental role played by chemotattractant receptors in pathologies such as rheumatoid arthritis, Crohn's disease, and ischemia-reperfusion injury, pharmacological targeting of FPR and C5aR or one of the effector molecules, might greatly alleviate the destructive effects of neutrophils.

Abbreviations used in this paper

FPR, formyl peptide receptor; C5aR, anaphylatoxin C5a receptor; GPCR, G protein-coupled receptor; fMLF, f-methionine-leucine-phenylalanine; EndoH, endoglycosidase H; PNGase F, N-glycosidase F; mAb, monoclonal antibody; CHO, Chinese h0061mster ovary; GRK, G protein-coupled receptor kinase; ERK1/2, extracellular signalregulated kinase 1/2.

Acknowledgments

We thank Ross Taylor and John Mills for helpful discussions and advice concerning structural studies of FPR, Robert Lefkowitz for antibody against β-arrestin1/2, Jim Burritt for immunofluorescence microscope usage, and Bruce Granger for critical reading of the manuscript. This study was supported by NIH grant R01 AI51726 (HMM) and American Heart Association Grant-in-Aid 060153Z (HMM). AJJ was supported by NIH grant R56 AI22735. The DNA sequencing was supported by NIH grant P20 RR-016464 from INBRE Program from the National Center for Research Resources (University of Nevada, Reno, NV).

References

1. Rabiet MJ, Huet E, Boulay F. The N-formyl peptide receptors and the anaphylatoxin C5a receptors: an overview. Biochimie 2007;89:1089. [PubMed: 17428601]
2. Gurevich VV, Gurevich EV. The structural basis of arrestin-mediated regulation of G-protein-coupled receptors. Pharmacol. Ther 2006;110:465. [PubMed: 16460808]
3. Suvorova ES, Gripentrog JM, Oppermann M, Miettinen HM. Role of the carboxyl terminal di-leucine in phosphorylation and internalization of C5a receptor. Biochim. Biophys. Acta 2008;1783:1261. [PubMed: 18346468]
4. Anelli T, Sitia R. Protein quality control in the early secretory pathway. EMBO J 2008;27:315. [PubMed: 18216874]
5. Marchese A, Paing MM, Temple BR, Trejo J. G protein-coupled receptor sorting to endosomes and lysosomes. Annu. Rev. Pharmacol. Toxicol 2008;48:601. [PubMed: 17995450]
6. Boulay F, Mery L, Tardif M, Brouchon L, Vignais P. Expression cloning of a receptor for C5a anaphylatoxin on differentiated HL-60 cells. Biochemistry 1991;30:2993. [PubMed: 2007135]
7. Gerard NP, Gerard C. The chemotactic receptor for human C5a anaphylatoxin. Nature 1991;349:614. [PubMed: 1847994]
8. Riesselman M, Miettinen HM, Gripentrog JM, Lord CI, Mumey B, Dratz EA, Taylor RM, Jesaitis AJ. N-formyl peptide receptor C-terminal tail phophorylation in the specific granule pool and after fMLF activation: Differential receptor recognition by monoclonal antibodies NFPR1 and NFPR2. J. Immunol 2007;179:2520. [PubMed: 17675514]
9. Boulay F, Tardif M, Brouchon L, Vignais P. The human N-formylpeptide receptor. Characterization of two cDNA isolates and evidence for a new subfamily of G-protein-coupled receptors. Biochemistry 1990;29:11123. [PubMed: 2176894]
10. Uthayakumar S, Granger BL. Cell surface accumulation of overexpressed hamster lysosomal membrane glycoproteins. Cell. Mol. Biol. Res 1995;41:405. [PubMed: 8867788]
11. Laemmli UK. Cleavage of structural protein during assembly of the head of bacteriophage T4. Nature 1970;222:680. [PubMed: 5432063]
12. Miettinen HM, Gripentrog JM, Mason MM, Jesaitis AJ. Identification of putative sites of interaction between the human formyl peptide receptor and G protein. J. Biol. Chem 1999;274:27934. [PubMed: 10488141]
13. Gripentrog JM, Miettinen HM. Activation and nuclear translocation of ERK1/2 by the formyl peptide receptor is regulated by G protein and is not dependent on β-arrestin translocation or receptor endocytosis. Cell. Signal 2005;17:1300. [PubMed: 16038804]
14. Key TA, Foutz TD, Gurevich VV, Sklar LA, Prossnitz ER. *N*-formyl peptide receptor phosphorylation domains differentially regulate arrestin and agonist affinity. J. Biol. Chem 2003;278:4041. [PubMed: 12424254]

15. Potter RM, Key TA, Gurevich VV, Sklar LA, Prossnitz ER. Arrestin variants display differential binding characteristics for the phosphorylated *N*-formyl peptide receptor carboxyl terminus. J. Biol. Chem 2002;277:8970. [PubMed: 11777932]

16. Potter RM, Maestas DC, Cimino DF, Prossnitz ER. Regulation of N-formyl peptide receptor signaling and trafficking by individual carboxyl-terminal serine and threonine residues. J. Immunol 2006;176:5418. [PubMed: 16622009]

17. Palczewski K, Kumasaka T, Hori T, Behnke CA, Motoshima H, Fox BA, Le Trong I, Teller DC, Okada T, Stenkamp RE, Yamamoto M, Miyano M. Crystal structure of rhodopsin: A G protein-coupled receptor. Science 2000;289:739. [PubMed: 10926528]

18. Cherezov V, Rosenbaum DM, Hanson MA, Rasmussen SG, Thian FS, Kobilka TS, Choi HJ, Kuhn P, Weis WI, Kobilka BK, Stevens RC. High-resolution crystal structure of an engineered human β2-adrenergic G protein-coupled receptor. Science 2007;318:1258. [PubMed: 17962520]

19. McGuffin LJ, Bryson K, Jones DT. The PSIPRED protein structure prediction server. Bioinformatics 2000;16:404. [PubMed: 10869041]

20. Fontana A, de Laureto PP, Spolaore B, Frare E, Picotti P, Zambonin M. Probing protein structure by limited proteolysis. Acta Biochim. Pol 2004;51:299. [PubMed: 15218531]

21. Suvorova ES, Gripentrog JM, Miettinen HM. Different endocytosis pathways of the C5a receptor and the N-formyl peptide receptor. Traffic 2005;6:100. [PubMed: 15634211]

22. Altenbach C, Klein-Seetharaman J, Cai K, Khorana HG, Hubbell WL. Structure and function in rhodopsin: mapping light-dependent changes in distance between residue 316 in helix 8 and residues in the sequence 60–75, covering the cytoplasmic end of helices TM1 and TM2 and their connection loop CL1. Biochemistry 2001;40:15493. [PubMed: 11747424]

23. Mielke T, Villa C, Edwards PC, Schertler GF, Heyn MP. X-ray diffraction of heavy-atom labelled two-dimensional crystals of rhodopsin identifies the position of cysteine 140 in helix 3 and cysteine 316 in helix 8. J. Mol. Biol 2002;316:693. [PubMed: 11866527]

24. Melkonian KA, Ostermeyer AG, Chen JZ, Roth MG, Brown DA. Role of lipid modifications in targeting proteins to detergent-resistant membrane rafts. Many raft proteins are acylated, while few are prenylated. J. Biol. Chem 1999;274:3910. [PubMed: 9920947]

25. Johnson JE, Cornell RB. Amphitropic proteins: regulation by reversible membrane interactions (review). Mol. Membr. Biol 1999;16:217. [PubMed: 10503244]

26. Prossnitz ER, Kim CM, Benovic JL, Ye RD. Phosphorylation of the *N*-formyl peptide receptor carboxyl terminus by the G protein-coupled receptor kinase, GRK2. J. Biol. Chem 1995;270:1130. [PubMed: 7836371]

27. Maestes DC, Potter RM, Prossnitz ER. Differential phosphorylation paradigms dictate desensitization and internalization of the N-formyl peptide receptor. J. Biol. Chem 1999;274:29791. [PubMed: 10514456]

28. Cai K, Klein-Seetharaman J, Farrens D, Zhang C, Altenbach C, Hubbell WL, Khorana HG. Single-cysteine substitution mutants at amino acid positions 306–321 in rhodopsin, the sequence between the cytoplasmic end of helix VII and the palmitoylation sites: sulfhydryl reactivity and transducin activation reveal a tertiary structure. Biochemistry 1999;38:7925. [PubMed: 10387034]

29. Ernst OP, Meyer CK, Marin EP, Henklein P, Fu WY, Sakmar TP, Hofmann KP. Mutation of the fourth cytoplasmic loop of rhodopsin affects binding of transducin and peptides derived from the carboxyl-terminal sequences of transducin alpha and gamma subunits. J. Biol. Chem 2000;275:1937. [PubMed: 10636895]

30. Swift S, Leger AJ, Talavera J, Zhang L, Bohm A, Kuliopulos A. Role of the PAR1 receptor 8th helix in signaling: the 7-8-1 receptor activation mechanism. J. Biol. Chem 2006;281:4109. [PubMed: 16354660]

31. Delos Santos NM, Gardner LA, White SW, Bahouth SW. Characterization of theresidues in helix 8 of the human β1-adrenergic receptor that are involved in coupling the receptor to G proteins. J. Biol. Chem 2006;281:12896. [PubMed: 16500896]

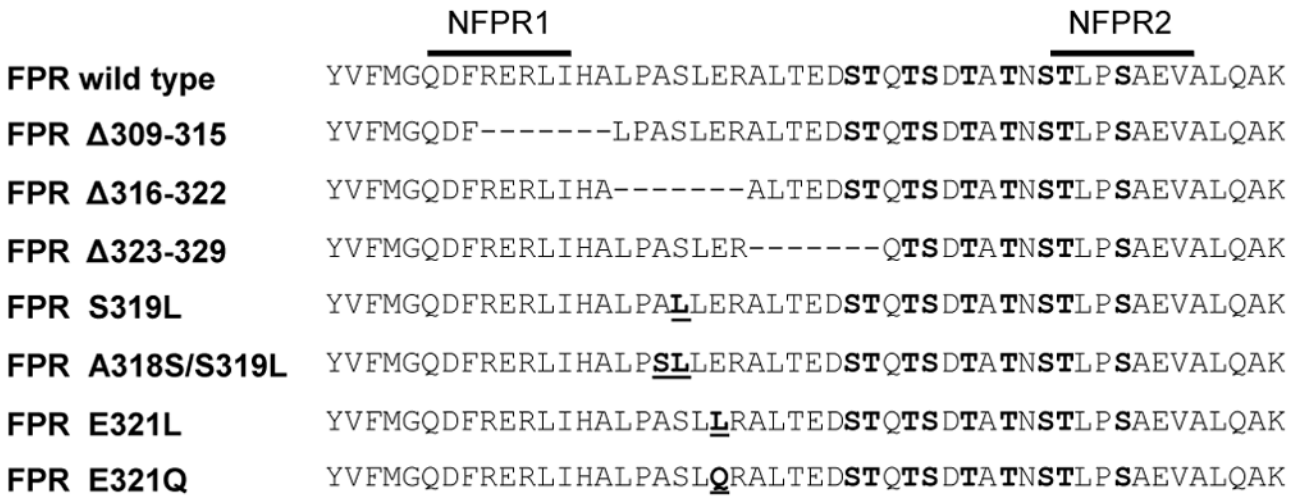

Figure 1. Amino acid sequences of wild type and mutant cytoplasmic tails of FPR

The serine and threonine residues in bold show the phosphorylation sites, as predicted by mutagenesis experiments [14]. The previously determined primary binding sites of two monoclonal antibodies, NFPR1 and NFPR2, are shown with lines above the amino acid sequence [8]. The deleted amino acids are indicated with a hyphen (-) and the mutated residues are in bold and underlined.

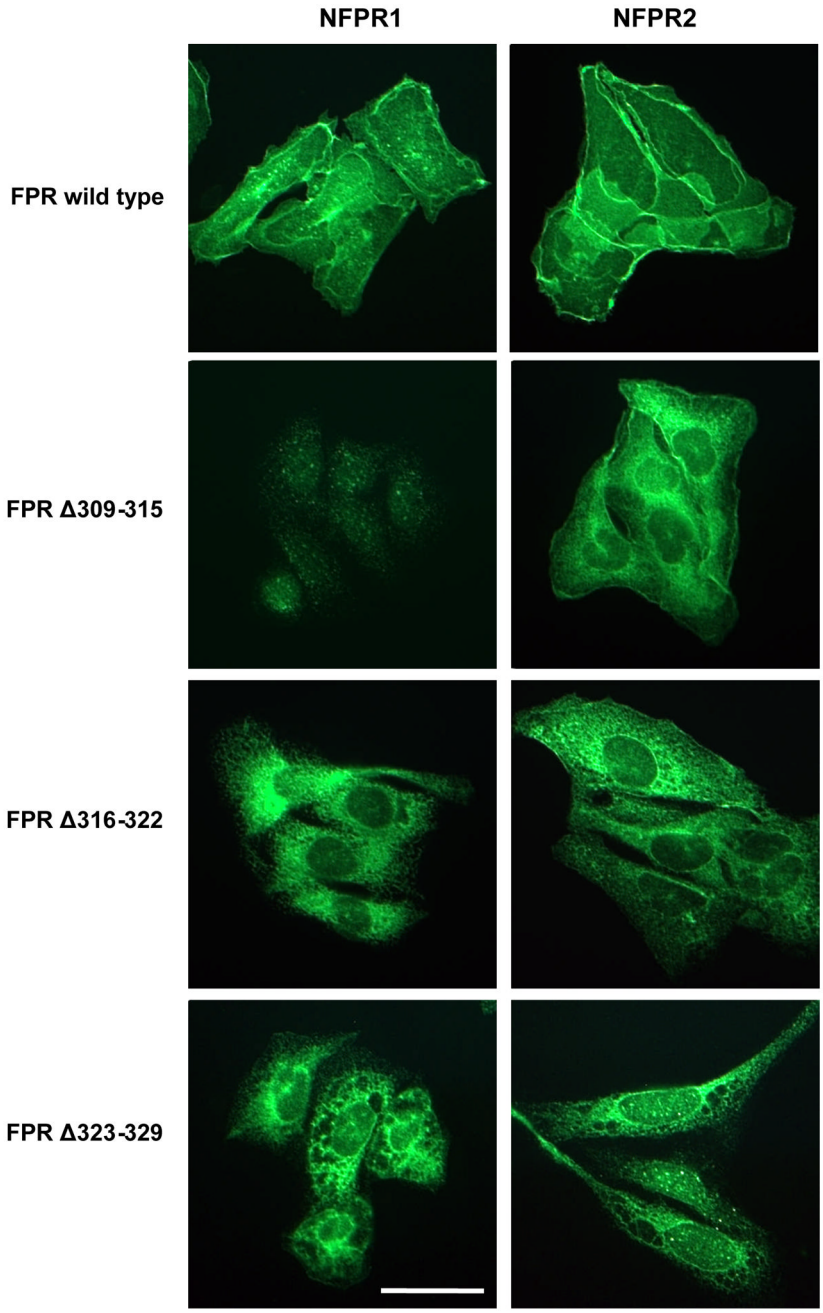

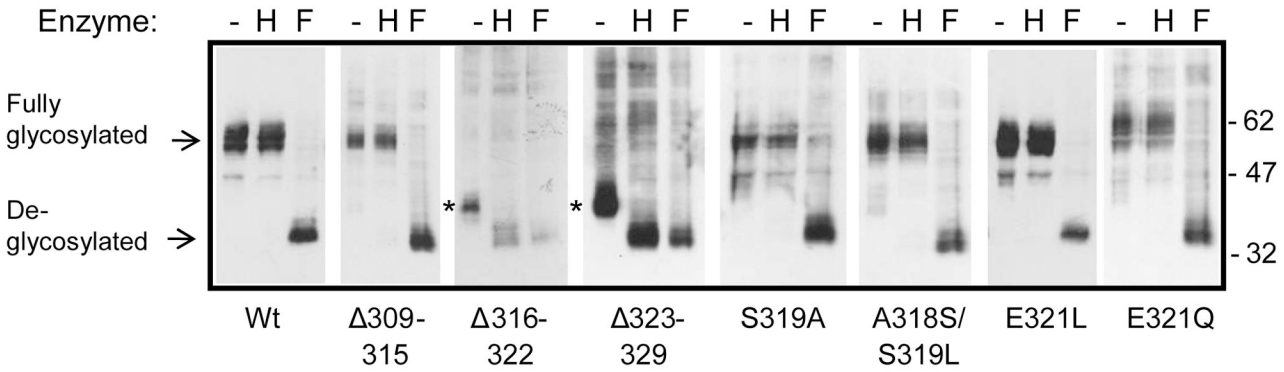

Figure 2. Two deletions of seven amino acids near the middle of the cytoplasmic tail of FPR result in protein retention in the endoplasmic reticulum

A) Immunofluorescence localization of wild type and mutant FPR in fixed and permeabilized CHO transfectants. FPR was stained with mAb NFPR1 (left column) or mAb NFPR2 (right column), followed by an Alexa™-488-conjugated secondary antibody. Bar 50 μm. B) Denatured cell extracts were incubated without enzyme (-) or in the presence of Endoglycosidase H (H) or PNGase F (F). FPR was detected in western blots with mAb NFPR2.

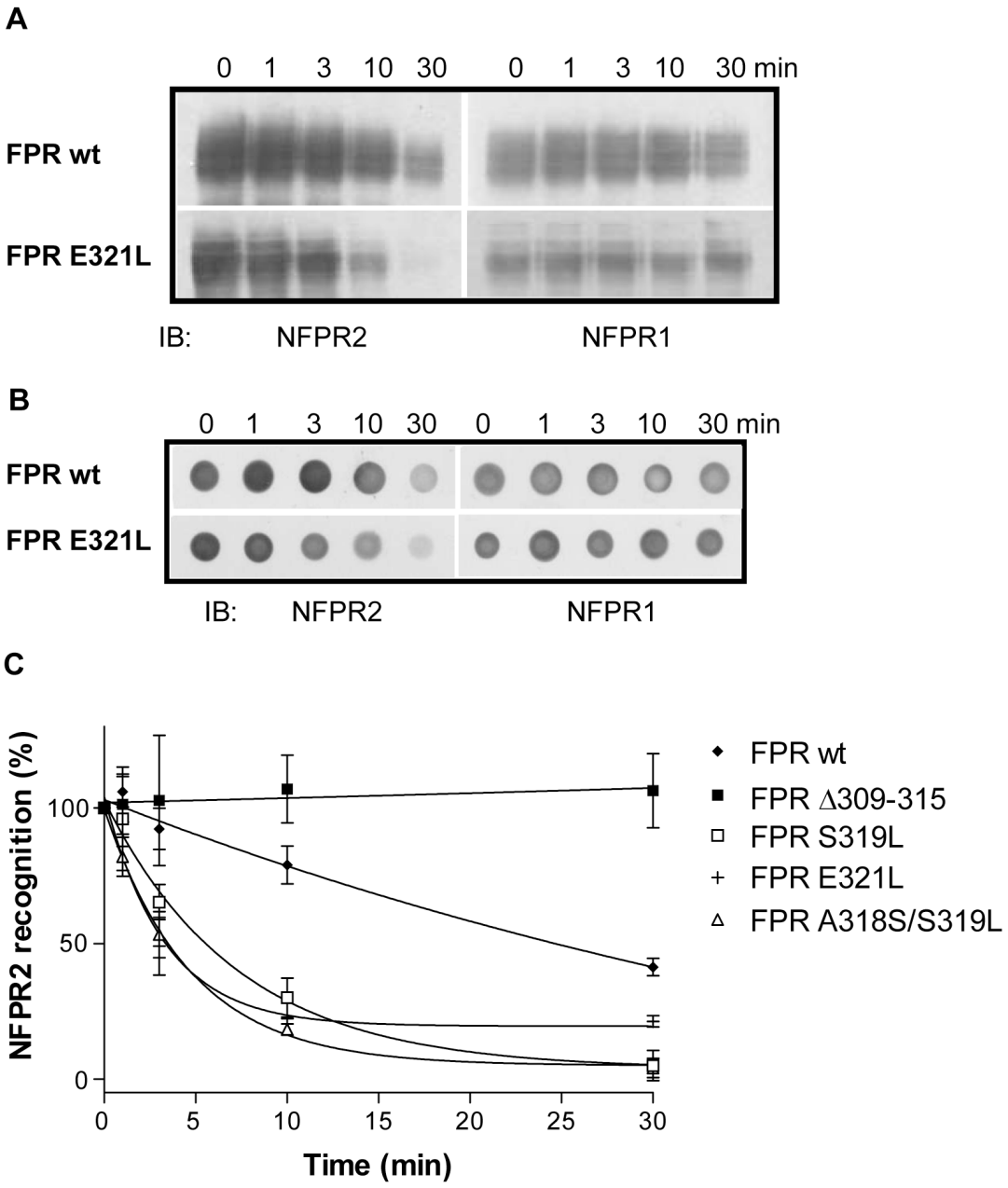

Figure 3. Wild type FPR shows a slower time course of receptor phosphorylation than the FPR mutants

A and B) Comparison of the time courses of agonist-induced phosphorylation of wild type FPR and the E321L mutant by western blot analysis. Cells were incubated for the indicated times with 100 nM fMLF. FPR was detected in conventional immunoblots (A) and dot-blots (B) with mAb NFPR2, which does not bind phosphorylated receptor, and mAb NFPR1, which binds both non-phosphorylated and phosphorylated receptor. C) Graphic representation of the increase in FPR phosphorylation shown as loss of mAb NFPR2 binding to the receptor. FPR phosphorylation was quantified from dot blots from a minimum of three experiments. The mean ± SD is shown for each time point.

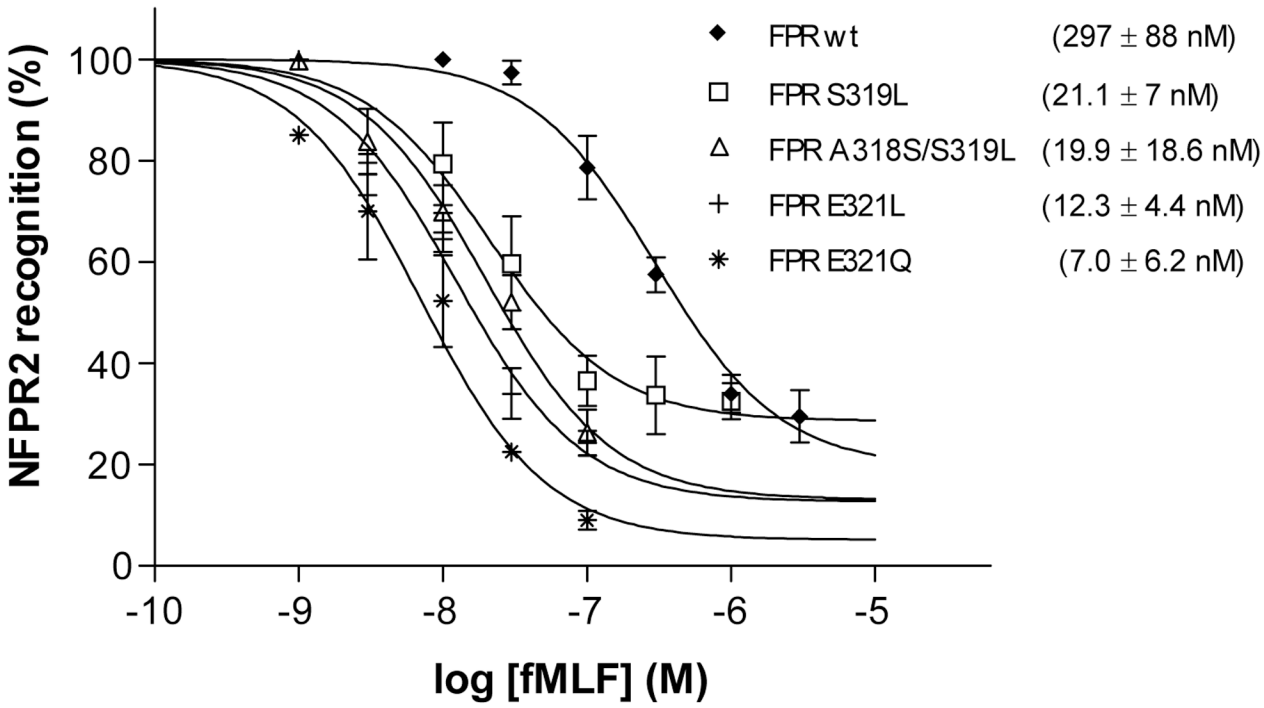

Figure 4. Wild type FPR requires a higher concentration of agonist for half maximal receptor phosphorylation than the FPR mutants

Western blot analysis of the concentration dependence of FPR phosphorylation. Cells were incubated for 5 min with various concentrations of fMLF as shown. FPR was detected as previously described (Figure 3). Non-linear regression analysis of mAb NFPR2 binding to wild type and mutant FPRs in the presence of various concentrations of ligand. EC_{50} is shown as mean ± SD from a minimum of three determinations.

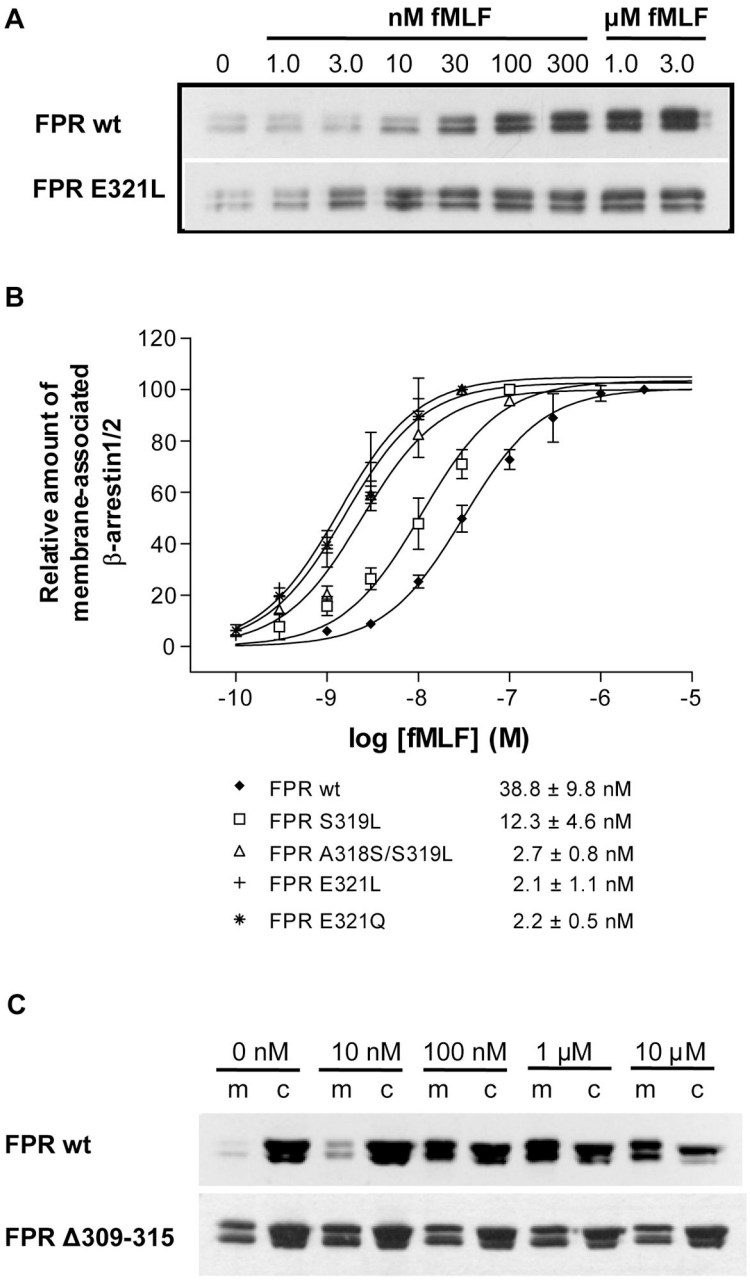

Figure 5. FPR point mutants show enhanced membrane translocation of ß-arrestin1/2 in response to agonist, whereas the FPR Δ309–315 mutant does not induce ß-arrestin1/2 translocation

A) Western blot analysis of fMLF-induced translocation of ß-arrestin1/2 to cell membranes from cells expressing wild type and mutant FPR. Cells were incubated for 5 min in the presence of various concentrations of fMLF. ß-Arrestin1/2 from membrane fractions was identified using a polyclonal antibody. B) Non-linear regression analysis of the fMLF concentration dependence of ß-arrestin1/2 membrane translocation. Results were obtained by scanning western blots from a minimum of three different experiments of each cell line. EC_{50} is shown as mean ± SD from a minimum of three determinations. C) The amount of ß-arrestin1/2 in the membrane fraction and the cytoplasmic fraction of CHO FPR wild type and Δ309–315 mutant

was compared. Cells were incubated for 5 min in the presence of various concentrations of fMLF, as shown. ß-Arrestin1/2 from membrane fractions (m) and cytoplasmic fractions (c) was identified using a polyclonal antibody, as above.

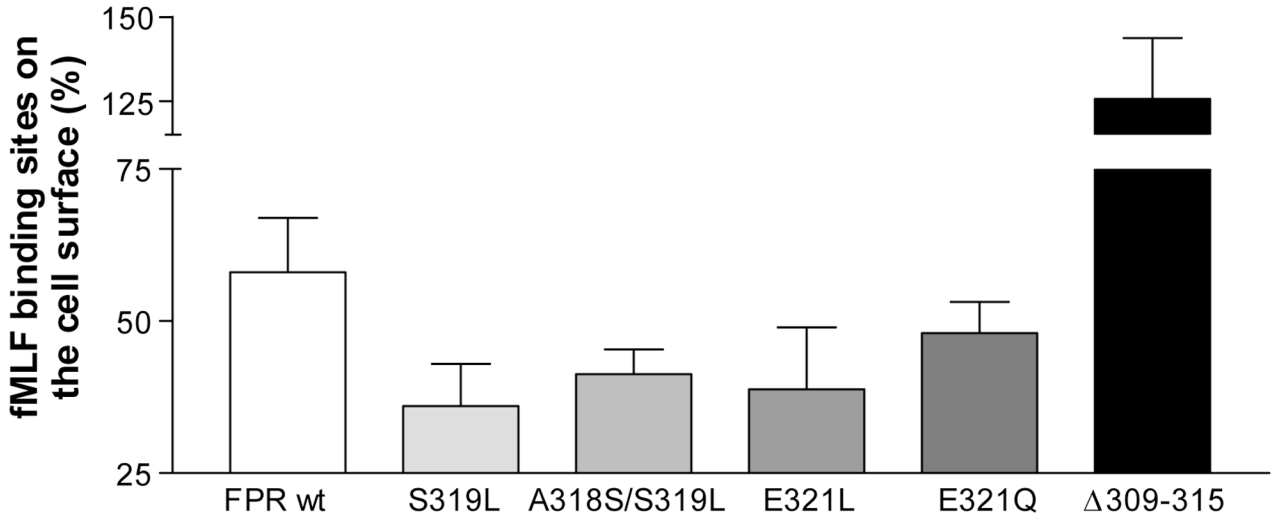

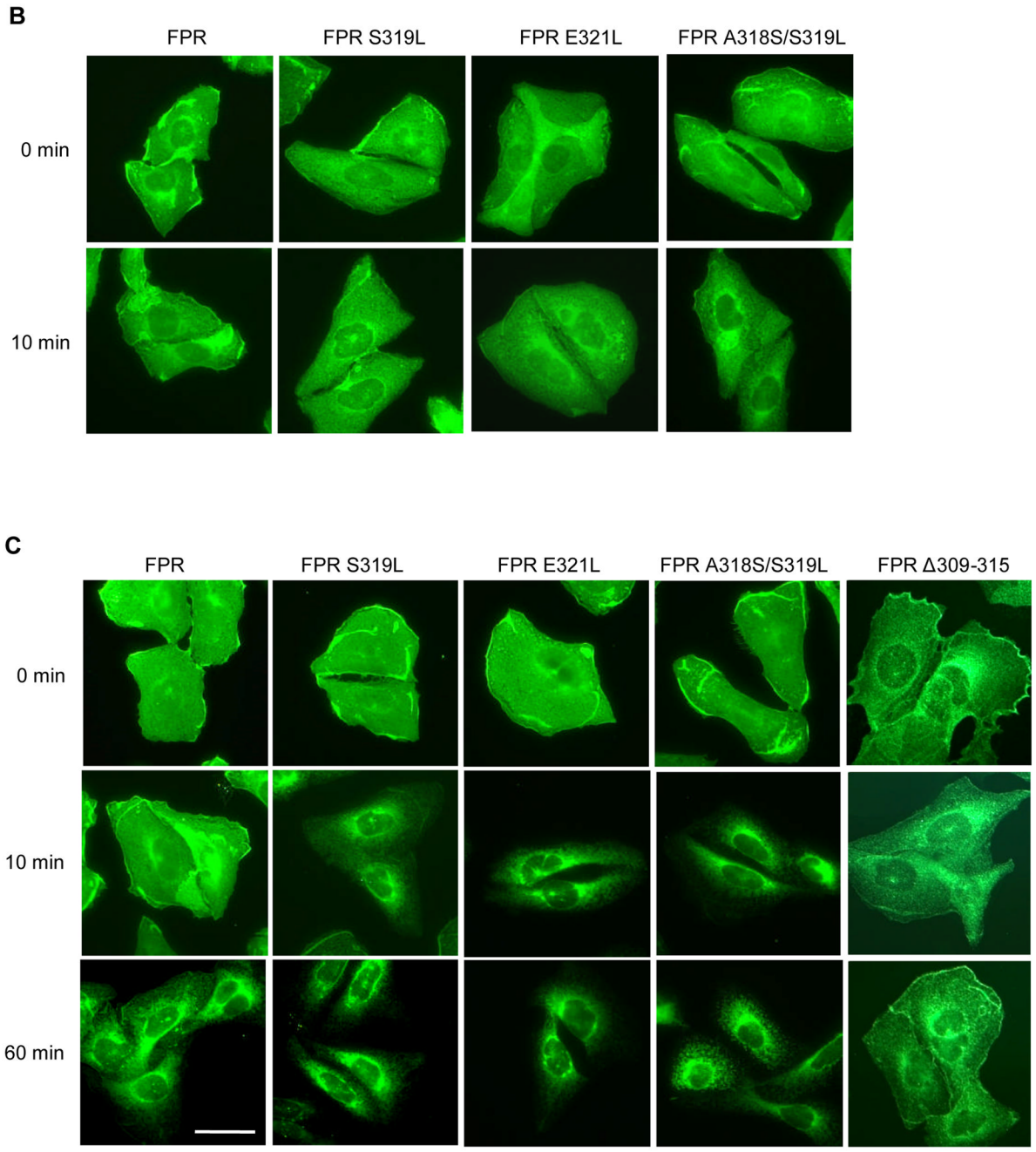

Figure 6. Enhanced receptor phosphorylation and ß-arrestin1/2 membrane translocation correlate with increased endocytosis

A) Flow cytometric analysis of endocytosed FPR. Cells were incubated for 15 min at 37°C in the presence or absence of 100 nM fMLF, washed to remove remaining ligand, and incubated with a fluorescent formylated hexapeptide to detect FPR remaining on the cell surface. The data are shown as percentage of binding sites on the cell surface, compared to cells incubated in the absence of fMLF. Data show means ± SD from a minimum of three different experiments. $P = 0.0057$ (non-parametric one-way ANOVA). B) Immunofluorescence analysis of total FPR after 0 or 10 min incubation with fMLF. Methanol fixed and permeabilized cells were incubated with mAb NFPR1 and fluorescent secondary antibody to stain total FPR. (Results for FPR

Δ309–315 are not shown since mAb NFPR1 does not bind the mutant receptor.) C) Immunofluorescence analysis of non-phosphorylated FPR after 0, 10 or 60 min incubation with fMLF. Methanol fixed and permeabilized cells were incubated with mAb NFPR2 and fluorescent secondary antibody to stain non-phosphorylated FPR. Bar 50 μm.

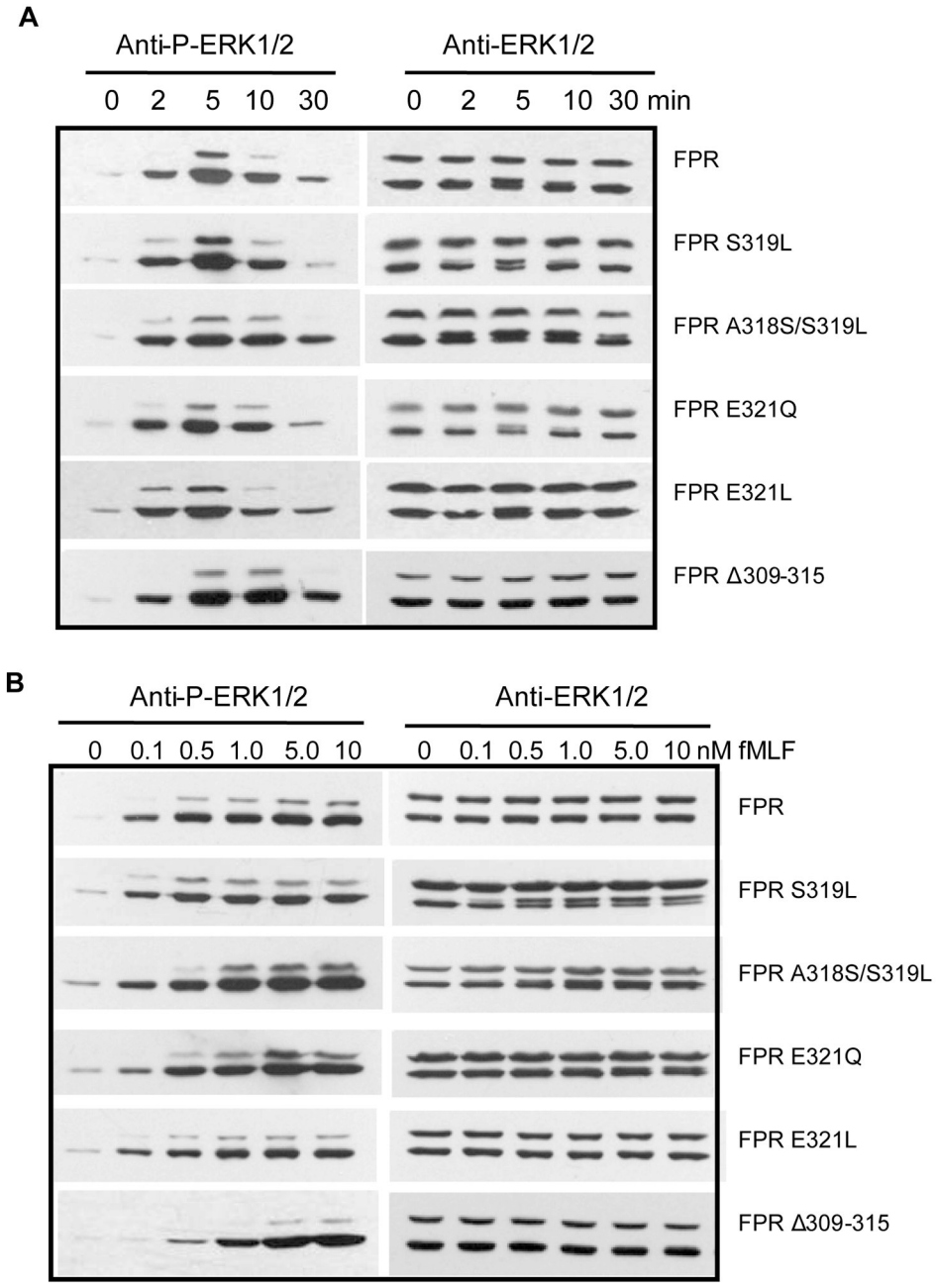

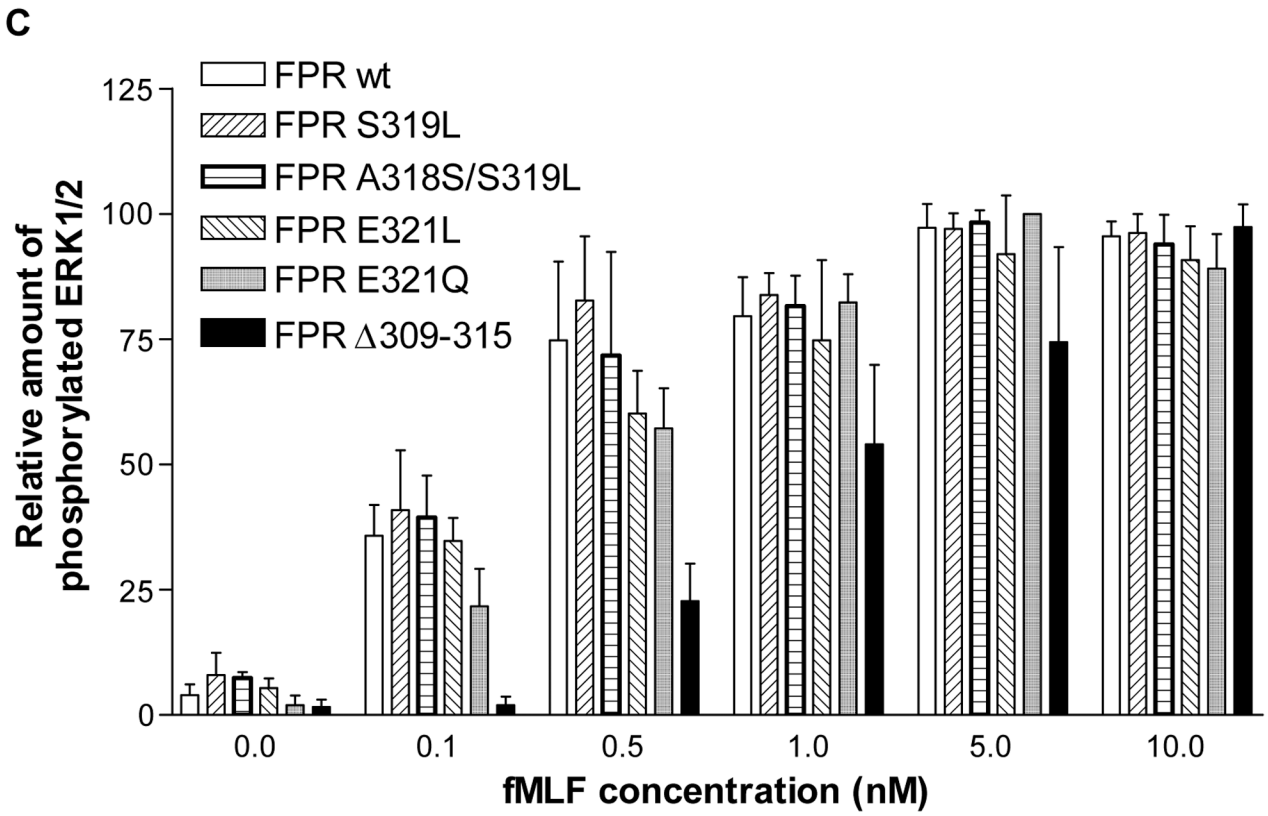

Figure 7. FPR point mutants show similar activation of ERK1/2 as wild type FPR

A) Western blot analysis of the time course of ERK1/2 activation. Cells were incubated in the presence of 100 nM fMLF for 0, 2, 5, 10 or 30 min. Phosphorylated ERK1/2 was visualized using an antibody that recognizes ERK1/2 phosphorylated on Thr202/Tyr204 (left column) and total ERK1/2 was visualized using an antibody that recognizes both non-phosphorylated and phosphorylated receptor (right column). B) Western blot analysis of the fMLF concentration dependence of ERK1/2 activation. Cells were incubated for 5 min with various concentrations of fMLF, as shown. Phosphorylated and total ERK1/2 was visualized as above. C) Quantification of the relative amount of phosphorylated ERK1/2 in response to 5 min incubation with various concentrations of fMLF. The results are means ± SD from a minimum of three different experiments for each receptor.

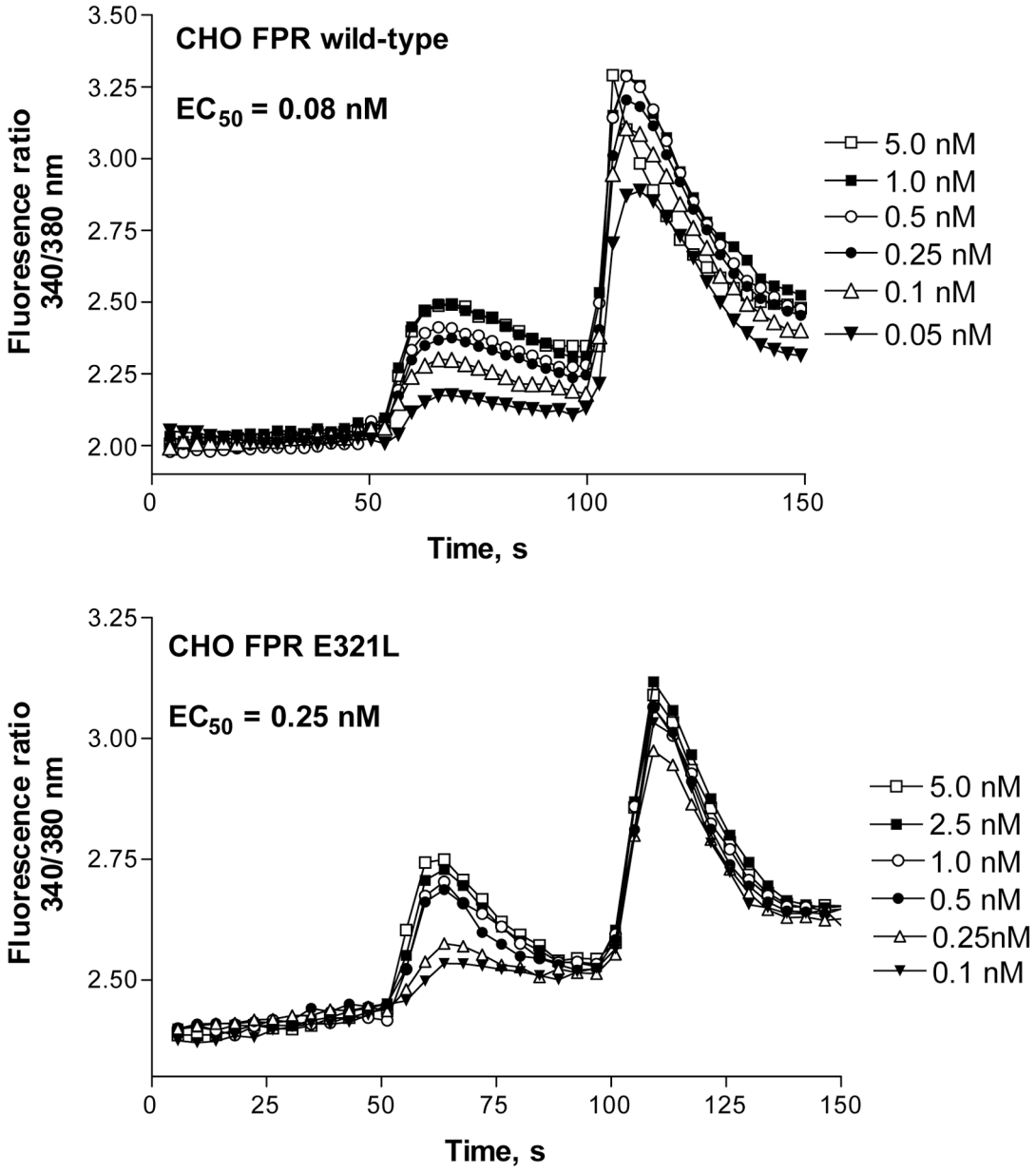

Figure 8. CHO FPR wild type and CHO FPR E321L show similar calcium curves in response to fMLF

Cells loaded with Fura 2-AM were induced to release intracellular calcium by the addition of various concentrations of fMLF at 50 s, as shown. 10 μM ATP was added at 100 s to provide a standard stimulus for calcium release.

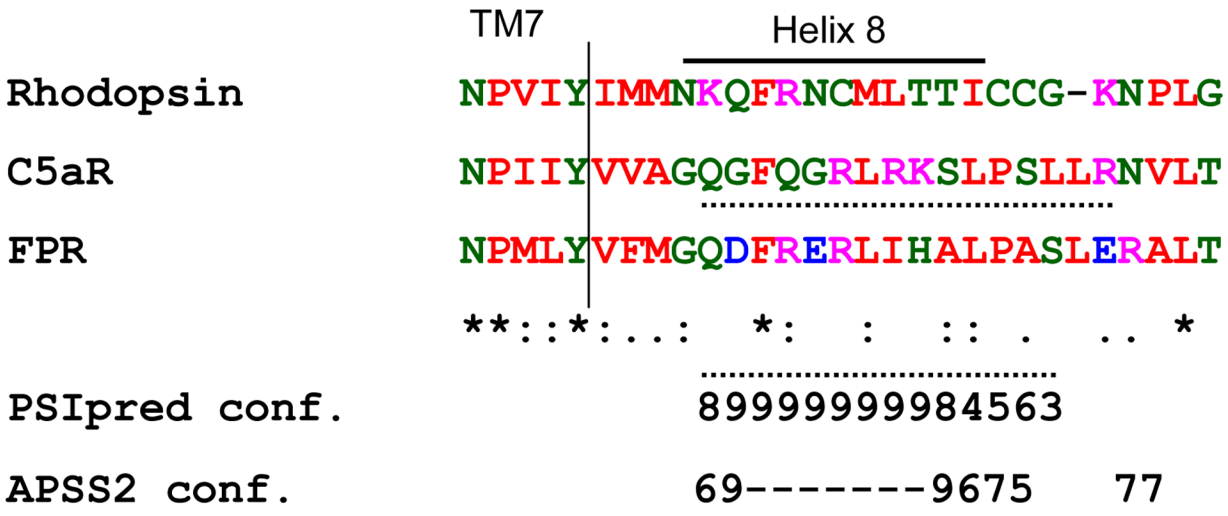

Figure 9. Computational prediction of the helical structure in the membrane proximal region of the cytoplasmic tail of FPR

Amino acid sequences of bovine rhodopsin (N301-G328), human C5aR (N296-T324) and human FPR (N297-T325) were aligned (vertical line) relative to the 7th transmembrane domain (TM7). The position of helix 8 of rhodopsin is based on the resolved crystal structure [17]. Star (*) indicates identical amino acids in all three sequences. Two dots (:) indicates tolerable amino acid substitutions, and one dot (.) indicates amino acid residues of similar size. The numbers underlying the sequences represent the rate of confidence for helical structure provided by PSIpred and APSS2 servers. Higher number stands for higher confidence. Hyphen (-) represents the highest confidence of 10, used in the APSS2 prediction. Dotted line (…..) underlines the sequence of the putative helix 8, as predicted by PSIpred and APSS2 analysis.

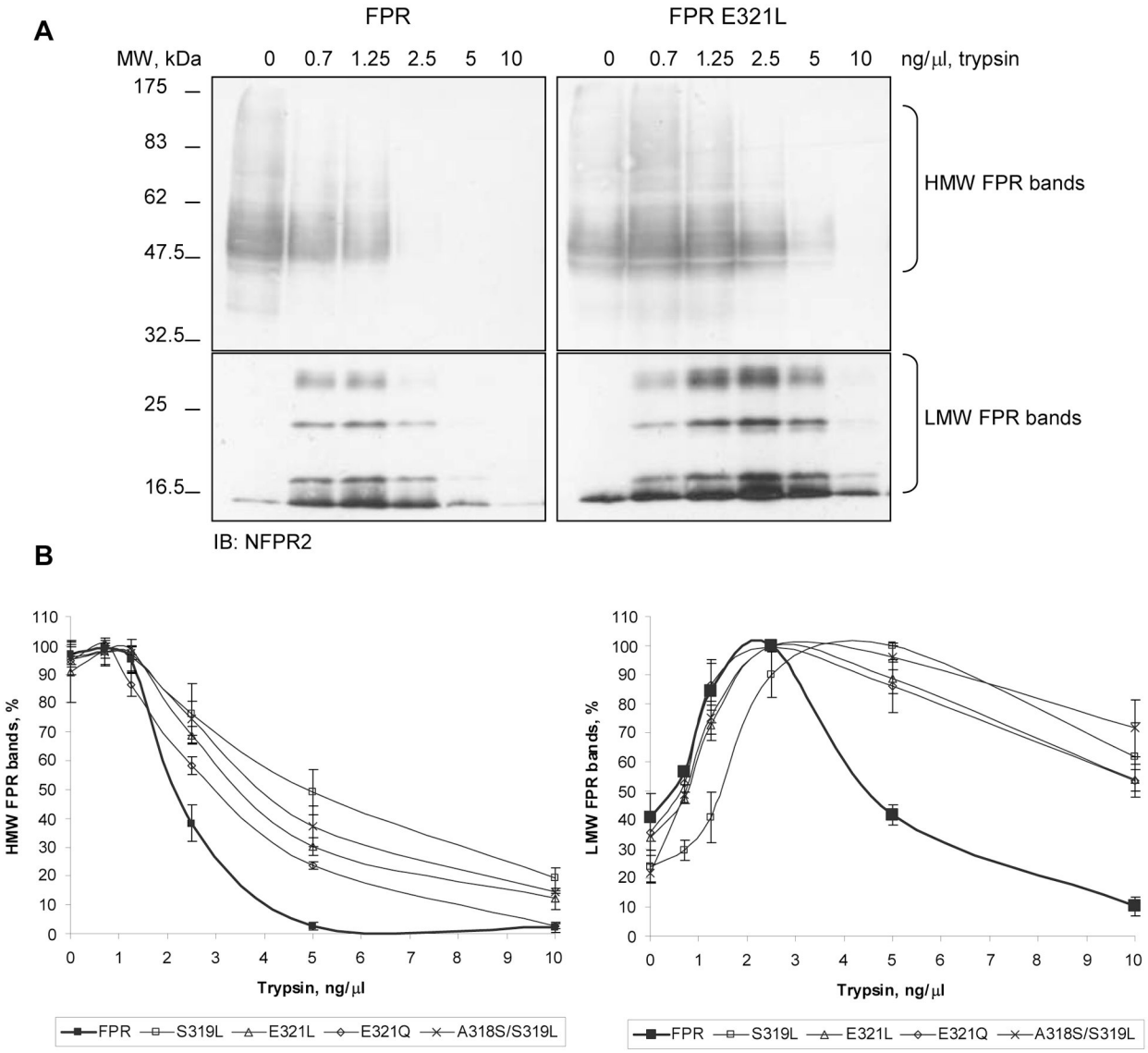

Figure 10. Wild type FPR is more susceptible to proteolysis than mutant FPRs

Triton X-100 solubilized membranes of CHO transfectants were treated with 0–10 ng/μl trypsin, as shown. Samples were analyzed in western blots using NFPR2 antibody. A) Representative western blots of the proteolysis of wild type FPR and FPR E321L mutant. B) Proteolysis was quantified from western blots by scanning. The graph on the left shows the decrease in the amount of intact and high molecular weight (HMW) FPR bands and the graph on the right shows the initial increase and the subsequent decrease in the amount of the proteolytic low molecular weight (LMW) FPR bands. The data are means ± SD from three different experiments.

Table 1

Cell surface expression and ligand binding affinity of wild type and mutant FPR

Receptor	Receptor localization	Cell surface expression (%)	K_d ± SD (nM)	Citation
FPR wild type	PM	100	6 ± 2.0	[12]
FPR Δ309–315	PM	18	2 ± 0.5	[12]
FPR Δ316–322	ER	N/A	N/A	[12]
FPR Δ323–329	ER	N/A	N/A	[12]
FPR A318S/S319L	PM	121	4 ± 1.6	This study
FPR S319L	PM	76	2 ± 0.5	This study
FPR E321L	PM	69	2 ± 0.7	This study
FPR E321Q	PM	78	3 ± 0.4	This study

Experiments were carried out as described in the Materials and Methods.

Abbreviations: PM, plasma membrane; ER, endoplasmic reticulum; N/A, not available.

Table 2

The EC_{50} values of fMLF-induced intracellular calcium release for wild-type and mutant FPR.

Receptor	EC_{50} (nM)
FPR wild type	0.11 ± 0.08
FPR S319L	0.11 ± 0.05
FPR E321L	0.22 ± 0.04
FPR E321Q	0.11 ± 0.12
FPR A318S/S319L	0.10 ± 0.05
FPR Δ309–315	1.70 ± 1.00